THE JOURNAL OF PHYSICAL CHEMISTRY B

Article

pubs.acs.org/JPCB

Dynamics of Formamide Ionic Solutions Investigated by Ultrafast Optical Kerr Effect

Francesca Palombo and Stephen R. Meech*

School of Chemistry, University of East Anglia, Norwich Research Park, Norwich NR4 7TJ, United Kingdom

Supporting Information

ABSTRACT: Molecular dynamics of formamide solutions of alkali metal halide salts were investigated using the time-resolved ultrafast optical Kerr effect (OKE) to observe the effects of ion solvation on the dynamics of a nonaqueous high-permittivity H-bonding solvent. The picosecond orientational and ultrafast intermolecular dynamics of liquid formamide as a function of concentration of NaI and KI are compared with the temperature effect on the pure solvent. The effect of a range of other salts at fixed concentration is also recorded. Transient OKE and corresponding low-frequency (THz) Raman spectra of the solutions revealed differences in the solvent dynamics caused by ion solvation. Increasing concentrations of NaI and KI have the effect of slowing down the diffusive reorientation and reducing the librational frequencies of formamide, with cation-related effects observed on the THz Raman spectrum. These effects are discussed in terms of an ion perturbation of the H-bonding structure in the solution. This approach provides a valuable means of investigating the dynamics, structure, and interactions in complex, interacting systems.

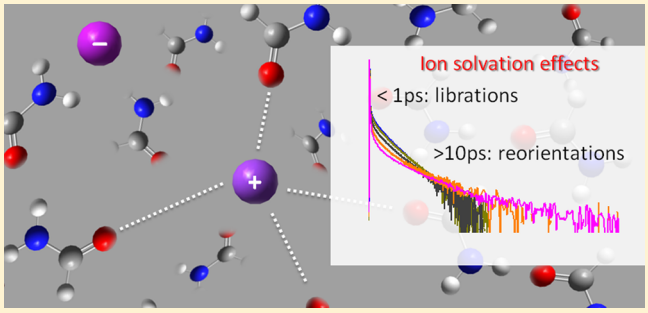

1. INTRODUCTION

Formamide (FA) is the simplest amide and, to some extent, a model for the peptide bond, especially in relation to the role of hydrogen (H)-bonding in the structure of peptides and proteins and to salt effects on them.[1] Liquid FA forms strong intermolecular H-bonds[2] (between the amide protons and the oxygen atom) and has a high dielectric constant, associated with the large molecular dipole moment (109.03 and 3.37 D,[3] respectively) which together make it a model solvent for nonaqueous electrolytes.[3] It also shows a high viscosity and low self-diffusion coefficient, which are indicative of a strong degree of association. These properties make it a good candidate for the study of nonaqueous solvation in an H-bonding environment. In this work, we investigate ion solvation by FA using the ultrafast optical Kerr effect (OKE), which provides simultaneously the picosecond relaxation dynamics and the Raman spectral density (equivalent to the depolarized Rayleigh−low-frequency anisotropic Raman spectrum) in the 1−400 cm^{-1} region.

The structure of liquid FA has been widely investigated, using both experimental[2,4−13] and theoretical approaches.[14−28] An extensive (2D) network formed by H-bond association has been found to give rise to interconnected cyclic dimers and linear chains. There has been less attention to the dynamics of liquid FA. Single-molecule and collective orientational relaxation times were determined by NMR[29,30] and depolarized Rayleigh scattering,[31] OKE,[32,33] and dielectric relaxation spectroscopy (DRS).[34,35] Good agreement has been found between these data and the results of molecular dynamics (MD) simulations.[26,36] Time-resolved OKE experiments also proved effective in giving an insight into ultrafast (subpicosecond) dynamics, with details on the time scale[32] and spectral distribution[33] of intermolecular modes in liquid FA and aqueous FA solutions.

Ion solvation has attracted a great deal of interest over the past decades, especially in relation to the effects of ion−solvent interactions and of ion association in nonaqueous dipolar solvents.[35,37,38] FA is a complex molecular liquid, owing to its H-bonding capability, with an extended H-bonded network topologically different from that of water.[13,28] The crystalline phase shows a 2D structure for FA[39,40] compared to a 3D one for water.[41] Alkali metal halides (MX) dissolve quite well in liquid FA in such a way that, owing to the high permittivity of the medium, ion pairing is minimized, while solvation effects are apparent. For example, the observed red shift of the IR spectral profile of N−H(D) stretching of FA upon addition of MX denotes an anion effect through the formation of ($NH\cdots X^-$) H-bonds.[42]

MD simulations have been employed to study structural and dynamic properties of FA both in the pure liquid state[17,18,21−23,28] and in aqueous solution.[26,27,36] Raman and OKE spectra in the low-frequency (THz) region[5,6,33,43] have been reproduced using a number of models.[22,23,26,27] In particular, based on previous findings from Raman experi-

Received: September 3, 2012
Revised: October 15, 2012
Published: October 22, 2012

 © 2012 American Chemical Society dx.doi.org/10.1021/jp3087418 | J. Phys. Chem. B 2012, 116, 13481−13489

ments[5,6,44] and ab initio calculations,[21] Torii and Tasumi related the presence of two distinct librational components at approximately 100 and 190 cm^{-1} to the dimensionality of the H-bonding in liquid FA, with two-dimensional H-bonding modes peaked at ∼190 cm^{-1} and one-dimensional at ∼100 cm^{-1};[22,23] the former is absent from the Raman spectra of *N*-methylformamide and acetamide.[45] Furthermore, Elola and Ladanyi investigated the polarizability anisotropy relaxation of FA in aqueous solution and provided a description of the bimodal Raman spectrum in terms of molecular pair correlations (∼200 cm^{-1}) and single-molecule (∼100 cm^{-1}) contributions.[26,27] These findings constitute the basis for the present study of the dynamics of ionic FA solutions. OKE spectroscopy is especially well suited to investigating the liquid-phase dynamics and low-frequency Raman spectra of molecular liquids and solutions,[46−49] and has previously been applied to study dynamics associated with aqueous ion solvation.[50,51] Here we extend these studies to the case of ion solvation by FA.

2. MATERIALS AND METHODS

2.1. Materials. Spectrophotometric grade FA (≥99% pure) and the alkali metal halides (≥99.5% pure) were purchased from Sigma-Aldrich and used as received. Solutions were prepared by weight in a drybox under nitrogen atmosphere; their molar concentration was obtained once the density had been determined (by weight of a known volume; Table 1). Viscosity of all samples was measured at room temperature using an Ubbelohde viscometer, with water as a reference (viscosity data from NIST[52]).

Table 1. Density (ρ) and Viscosity (η) of Alkali Metal Halide−FA Solutions

	x	c/M	ρ/g mL^{-1}	η/cP
formamide			1.14	3.63
LiCl	0.051	1.33	1.17	6.89
NaCl	0.028	0.69	1.15	4.06
KCl	0.040	1.00	1.17	4.47
LiBr	0.050	1.28	1.22	6.68
NaBr	0.050	1.28	1.23	7.47
KBr	0.050	1.27	1.24	5.81
LiI	0.050	1.27	1.26	6.33
NaI	0.011	0.29	1.17	4.19
NaI	0.050	1.26	1.27	7.20
NaI	0.094	2.37	1.39	13.4
NaI	0.14	3.57	1.51	34.7
KI	0.010	0.25	1.18	3.90
KI	0.050	1.24	1.28	5.49
KI	0.10	2.48	1.41	8.63
KI	0.15	3.66	1.55	15.2

2.2. Optically Heterodyne Detected (OHD)-OKE Spectroscopy. OHD-OKE measurements were performed using the experimental setup previously described.[53] The source was a home-built Kerr lens mode-locked Ti:sapphire laser cavity,[54] which emitted 35 fs Gaussian pulses centered at 810 nm, with a 200 mW output power and 68 MHz repetition rate.

For each sample, the OKE signal ($S(t)$), which is a convolution of the photoinduced transient birefringence of the sample ($R(t)$) with the instrument response ($G^{(2)}(t)$, cross-correlation of the pump and probe pulses), was measured over a wide time range, up to 200 ps, hence allowing the detection of ultrafast (subpicosecond) librational to slower (tens of picoseconds) reorientational dynamics of the liquid. Measurements were made with a resolution of 20 fs/step in the interval −3 to −0.2 ps (to determine the background), 4 fs/step between −0.2 and 0.2 ps, then 10 fs/step between 0.2 and 0.4 ps, and 100 fs/step between 0.4 and 90 ps. For NaI and KI solutions at high concentration, measurements were extended to 200 ps, with a 1 ps step in the interval 120−200 ps.

Measurements of pure liquid FA were performed at different temperatures, in the range 5.0−65.0 °C, controlled through a circulating water bath, with a precision of ±0.1 °C. Experiments on salt solutions were performed at constant temperature, 25.0 (±0.1)°C, using freshly prepared solutions of 0.05 mole fraction x (c = 1.3 M). These solutions were filtered through a 0.20 μm Millipore Millex-LG PTFE filter and transferred into an optical quality fused silica cell. Saturated solutions were obtained with NaCl and KCl (c ∼ 0.69 and 1.0 M, respectively) as these are only sparingly soluble in FA. For two selected salts of higher solubility, NaI and KI, experiments were performed at a range of concentrations.

2.3. Data Analysis. The measured Kerr transient for liquid FA and its ionic solutions contains an instantaneous response due to the electronic hyperpolarizability (of a width which reflects the laser pulse autocorrelation), followed by a nuclear response which contains the liquid-phase dynamics of interest (Figure 1). In the following, we assume that the molecular FA response dominates the measured OKE because of its relatively large polarizability anisotropy[27] and its high concentration relative to the ions. In this way, we neglect the possible interaction-induced contributions to the response, but these are generally weak when the polarizability anisotropy is large.[55] The nuclear response reveals oscillatory nonexponential dynamics on the subpicosecond time scale. On the picosecond time scale, a nonexponential monotonically decreasing signal is observed which relaxes on the picosecond to tens of picoseconds time scale. This picosecond relaxation of the time response $R(t)$, which is the negative time derivative of the off-diagonal terms (anisotropy) of the polarizability tensor, was analyzed for each sample using a stretched exponential for the anisotropic polarizability correlation function.[56−58] Fit analysis had a starting point at ∼2 ps, avoiding the oscillatory ultrafast response (Figure 2). A number of factors can lead to a stretched exponential decay function, including dynamics associated with glassy relaxation or an inhomogeneous distribution of exponential decay times. Parameters of the fit function

$$R(t) = A\beta(t^{\beta-1}/\tau^{\beta}) \exp[-(t/\tau)^{\beta}]$$

were the amplitude factor A, the relaxation time τ, and the stretching coefficient β (=1 for exponential decay), which measures the deviation from the simple exponential case. An average relaxation time $\langle\tau\rangle$ was derived from $\langle\tau\rangle = (\tau/\beta)\Gamma(1/\beta)$, where Γ is the standard gamma function.[58] A sum of three exponential functions gave only a slightly worse result in terms of the distribution of residuals than the stretched exponential, but more fitting parameters were required.

To obtain the Raman spectral density separated from the picosecond dynamics, which contribute a spike near zero frequency, each stretched exponential function resulting from the fit analysis was subtracted from the corresponding Kerr transient data, prior to a Fourier transform deconvolution.[33,48,59] The imaginary part of the Fourier transform, which contains information on the nuclear dynamics, now corresponds to a reduced depolarized Rayleigh−low-frequency

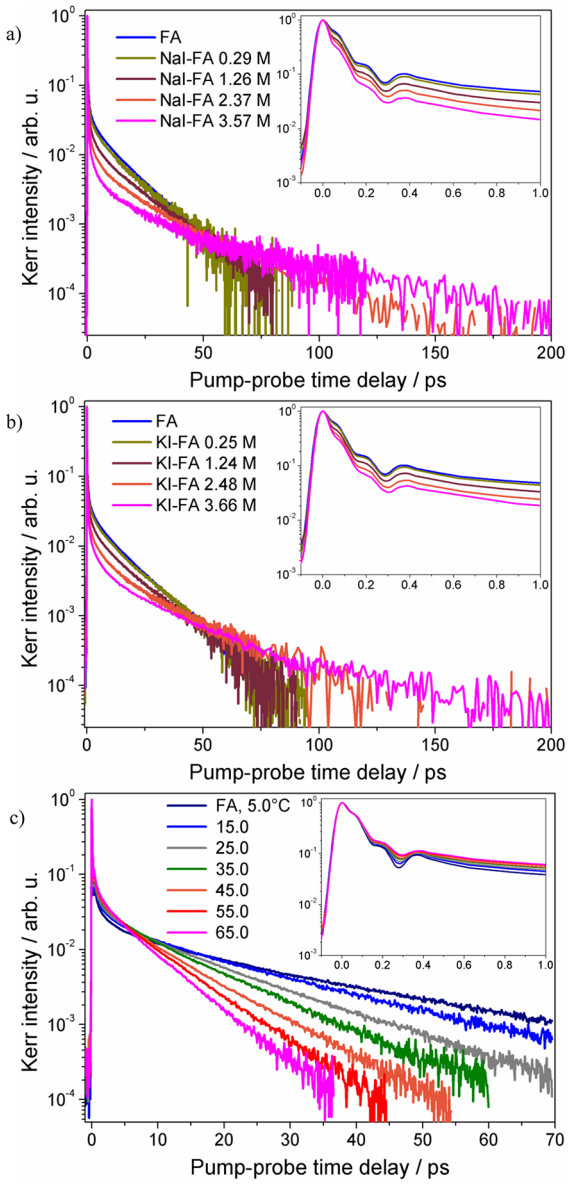

Figure 1. Evolution of the Kerr transient of (a) NaI–FA and (b) KI–FA solutions as a function of concentration, in the range 0–3.7 M, compared with that of the (c) pure liquid FA as a function of temperature, in the range 5.0–65.0 °C. Each data set was normalized to the electronic signal (t = 0). Inset: ultrafast part of the time-domain response, with the characteristic oscillations due to librational motions.

anisotropic Raman spectrum corrected for the Bose–Einstein occupation factor.[60] Hereafter we will refer to the resulting profile as a reduced Raman spectral density (rRSD) of the liquid. Each spectrum was subsequently decomposed by fit analysis in the range 0.03–400 cm^{-1} (Figure 3, and Figure SI-5 in the Supporting Information), using a sum of an ohmic, O, and two antisymmetrized Gaussian functions, G_1 and G_2 (Supporting Information, Table SI-I). This was the minimum set of modes required to accurately fit the experimental data (Figure 3).

3. RESULTS AND DISCUSSION

3.1. Picosecond Relaxation. Figure 1 shows the evolution of the Kerr transient decay of (a) NaI–FA and (b) KI–FA solutions as a function of concentration, in the range up to 3.7

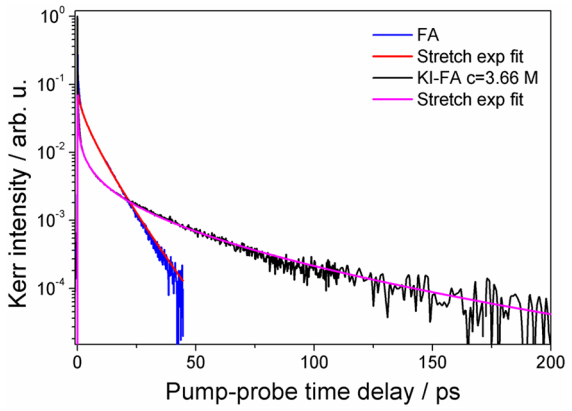

Figure 2. Normalized Kerr transient data for pure FA and a concentrated KI–FA solution, at 25.0 °C, with the stretched exponential fits shown (t > 2 ps).

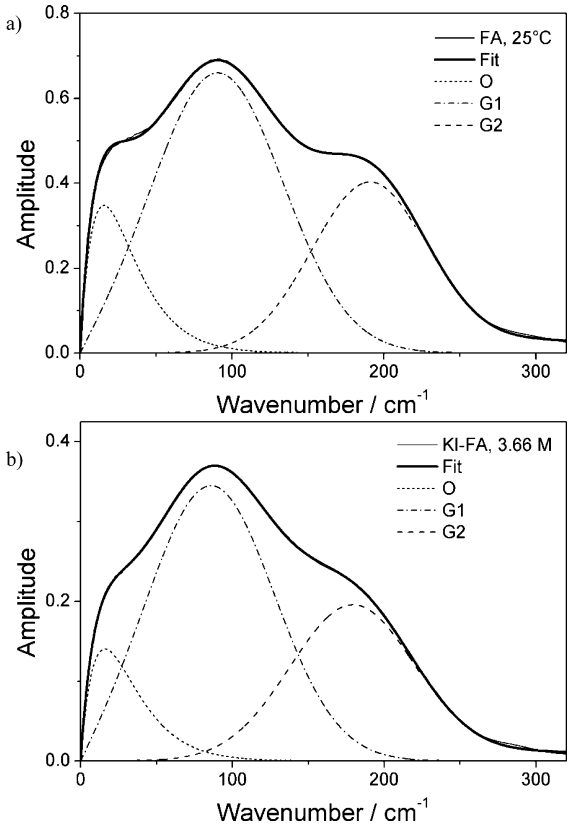

Figure 3. Results of a multicomponent fit applied to the rRSD of (a) pure FA and (b) a concentrated KI–FA solution, at 25.0 °C, using a sum of an ohmic and two antisymmetrized Gaussian functions.

M, at 25.0 °C. All transients were normalized to the electronic hyperpolarizability response, at t = 0. A slight change in the underdamped oscillatory features at very short times (inset) is observed with increasing concentration; the fastest damping becomes faster with increasing concentration and the oscillations become slightly less well pronounced. These changes are discussed further in the frequency domain analysis below. For longer times (>2 ps) as the ion concentration increases the amplitude of the fast relaxation becomes larger, but the slowest relaxation becomes slower, which overall gives rise to an increasing mean time associated with the stretched exponential relaxation (Table 2). It is interesting to compare

dx.doi.org/10.1021/jp3087418 | J. Phys. Chem. B 2012, 116, 13481–13489

Table 2. Parameters[a] of the Stretched Exponential Fit Applied to the Kerr Transient of (a) Alkali Metal Halide−FA Solutions at 25.0 °C, and (b) Pure FA at Different Temperatures

	(a) Alkali Metal Halide−FA Solutions at 25.0 °C			
	c/M	A	β	$\langle\tau\rangle$/ps
FA		0.42	0.82	12.70
LiCl	1.33	0.35	0.75	18.94
NaCl	0.69	0.36	0.80	14.24
KCl	1.00	0.40	0.79	14.93
LiBr	1.28	0.32	0.78	16.00
NaBr	1.28	0.32	0.74	17.85
KBr	1.27	0.36	0.74	17.70
LiI	1.27	0.32	0.75	17.32
NaI	0.29	0.36	0.81	12.98
NaI	1.26	0.27	0.76	15.84
NaI	2.37	0.20	0.68	21.80
NaI	3.57	0.16	0.57	43.30
KI	0.25	0.39	0.80	13.34
KI	1.24	0.29	0.78	14.36
KI	2.48	0.23	0.67	21.24
KI	3.66	0.19	0.60	30.23
	(b) Pure FA at Different Temperatures			
	T /°C	A	β	$\langle\tau\rangle$/ps
FA	5.0	0.50	0.77	25.85
	15.0	0.48	0.79	18.44
	25.0	0.42	0.82	12.70
	35.0	0.40	0.83	9.98
	45.0	0.36	0.85	7.73
	55.0	0.35	0.86	6.32
	65.0	0.33	0.86	5.32

[a]Values are reported as A, pre-exponential coefficient; β, stretching parameter; and $\langle\tau\rangle$, average relaxation time (see text).

the effects of increasing salt concentration to that of decreasing temperature for the pure solvent (Figure 1c). Neat FA presents a marked slowdown in the picosecond relaxation with decreasing temperature from 65.0 to 5.0 °C. This is qualitatively similar to the effect of increasing ion concentration (Figures 1a,b). However, in contrast to the case of ion solvation the effect of decreasing temperature on the oscillatory response is smaller, mainly the oscillations become slightly more pronounced at lower temperature; no such effect is evident at higher ion concentration (Figure 1a,b).

Previous research on unassociated liquids has shown that the slowest relaxation measured in OHD-OKE experiments scales with viscosity and can be ascribed to diffusive molecular reorientation.[49,61−64] To investigate this possibility for FA and its ionic solutions, their viscosities were measured (Table 1). All Kerr transients were non-single exponential over the wide time range of the measurements. However, a single stretched exponential function accurately reproduced the observed relaxation, providing an average relaxation time $\langle\tau\rangle$ of the liquid (Table 2). Data for pure liquid FA showed an increase of $\langle\tau\rangle$ with decreasing temperature (Table 2b) and increasing viscosity, consistent with progressively slower reorientational dynamics of the liquid. For the ionic solutions (Table 2a), the mean relaxation time increased as the concentration increased. However, the increase was a function of the dissolved ion, with a slightly greater slowdown being observed for Na^+ than for K^+. This trend was reproduced for other salts (see Supporting Information, Figure SI-1), with a slightly stronger effect of Na^+ than K^+ in both bromide and iodide solutions at c = 1.3 M. This effect is more clearly evident from the data for the NaI and KI solutions at higher concentrations (Table 2a), showing that $\langle\tau\rangle$ becomes more than twice the value in pure FA, but significantly (~40%) longer for NaI than KI. Figure 4(a) is a plot of the

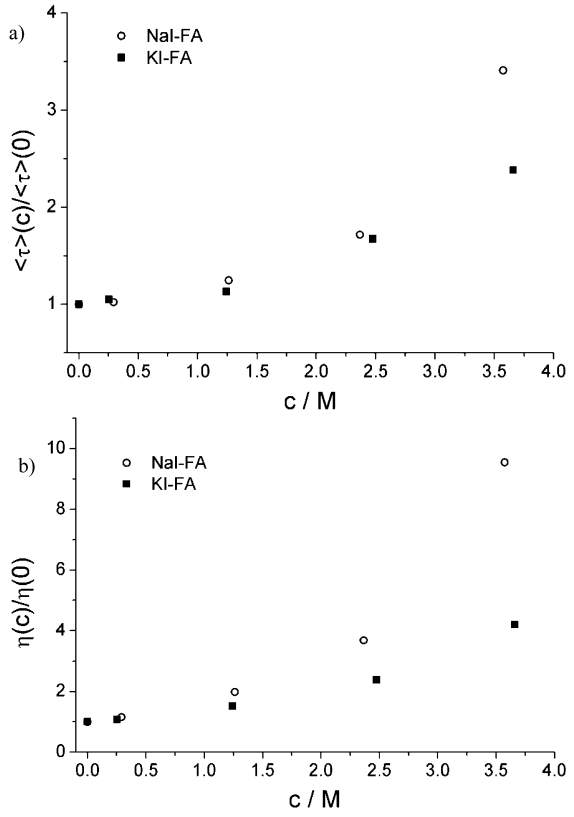

Figure 4. Plot of (a) relative average relaxation time, derived from fitting the Kerr transient of NaI and KI−FA solutions to a stretched exponential, and (b) relative viscosity of the same solutions versus concentration. Error bars are within the symbol size.

relative times $\langle\tau\rangle(c)/\langle\tau\rangle(0)$ in NaI and KI−FA solution as a function of concentration. The $Na^+ > K^+$ effect observed on the relaxation time is also reflected in the viscosity of the liquid, which has the order η(NaI) > η(KI), as shown in Figure 4b.

The value of $\langle\tau\rangle$ for pure liquid FA and its temperature dependence (Table 2b) are in good agreement with previously obtained results.[31−34] In particular, $\langle\tau\rangle$ at 25.0 °C (12.70 ps) proved to be close to the value of τ_1 (slower time) from a biexponential fit to the Kerr transient decay of FA.[32,33] Indeed, the stretching parameter that we obtained for pure FA is rather close to unity (β = 0.82 for FA at 25 °C; Table 2). Also, the $\langle\tau\rangle$ recovered at the different temperatures for pure FA are similar to the data previously derived using dielectric relaxation spectroscopy (DRS),[34] provided the 1/3 correction for the different ranks of the orientational correlation function probed by DRS and OKE is taken into account. This supports the assignment of $\langle\tau\rangle$ to the diffusive reorientation dynamics of liquid FA, as also indicated by the linearity of the Stokes−Einstein−Debye (SED) plot in Figure 5. In liquid FA, diffusion will be restricted by H-bonding interactions, unlike the case for unassociated liquids. Accordingly, $\langle\tau\rangle$ can be treated as arising from an activated process associated with weakening H-bonds. From the present data we recover an activation energy of 6.5 ± 0.4 kcal mol^{-1} from a simple Arrhenius analysis; this is close to

dx.doi.org/10.1021/jp3087418 | J. Phys. Chem. B 2012, 116, 13481−13489

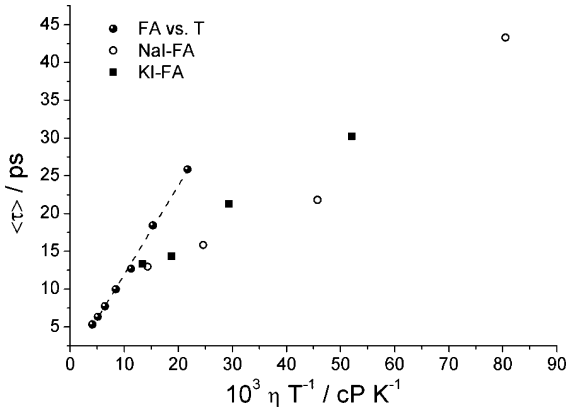

Figure 5. Stokes–Einstein–Debye plot of the average relaxation time derived from stretched exponential fits to the Kerr transients of (filled circles) pure FA at different temperatures, and (empty circles) NaI and (filled squares) KI–FA solutions at different concentrations, at 25.0 °C. Error bars are within the symbol size. Dashed line is a linear fit to the pure solvent data (R^2 = 0.998).

the energy associated with a single NH···O=C bond.[65] This is also similar to the activation energy for viscous flow in liquid FA, 5.3 ± 0.2 kcal mol^{-1}, derived from data in ref 66; this underlines the link between macroscopic viscosity and microscopic relaxation which exists even for the associated FA liquid.

Overall, slower dynamics (i.e., longer $\langle\tau\rangle$) are found for the MX–FA solutions (Table 2a), particularly at higher electrolyte concentrations (Figure 4a). Both the density and viscosity of liquid FA are found to increase upon addition of salt (Table 1), consistent with a change in solvent structure due to the ion–molecule interactions. An increased viscosity is in line with positive values of the Jones–Dole B coefficients already reported for these salts in more dilute FA solution ($c \leq 0.05$ M),[67] denoting a structure-making effect of the solute. It is interesting to note that both structure-making and -breaking effects are reported for these ionic solutes in water.[68,69] The above-noted differential effect of Na^+ and K^+ (Figure 4b) on η is consistent with NaI having a higher B coefficient. The B coefficient in the Jones–Dole expression for electrolyte solutions accounts for ion–solvent interactions and depends on the ion size. It has previously been found that $B(Na^+) > B(K^+)$ in dilute FA solution,[70] hence supporting a structure-making effect of the cation in the order Na^+ ($>Li^+$) > K^+. This is reproduced through our observed viscosities at constant concentration (Table 1), as well as at the higher concentrations of NaI and KI (Figure 4b). The stronger effect of NaI compared to KI on viscosity of liquid FA, which was noted in the corresponding $\langle\tau\rangle$ values at the highest concentration (Figure 4a), indicates an important cation effect on the solution dynamics ($Na^+ > K^+$).

Figure 5 also includes a SED plot of $\langle\tau\rangle$ for the NaI and KI–FA solutions, which can thus be compared to the data for liquid FA at different temperatures. Clearly, $\langle\tau\rangle$ for the solutions has a weaker η/T dependence than the corresponding time for the pure solvent, indicating a different reorientation mechanism (or activation parameter). This is also evident in Figure 4, with η (Figure 4b) increasing more than $\langle\tau\rangle$ (Figure 4a) with increasing ion concentration. For pure FA, a linear fit of $\langle\tau\rangle$ versus η/T has a smaller slope than that predicted by the SED using a molecular volume calculated from the density. This is also the case for many dipolar aprotic solvents and correction coefficients are required to take into account the shape of the rotating particle and boundary conditions.[71] In addition, OKE measures a *collective* relaxation time (τ_c), which is related to the single-molecule relaxation time (τ_{sm}) by the ratio g_2/j_2 (where g_2 and j_2 are respectively the static and dynamics pair correlation parameters, the latter usually taken as ≈1, such that $\tau_c = \tau_{sm}g_2$; see refs 45, 48, 49, 60, and 72). Single-molecule rotational times of FA are unavailable for all samples and conditions examined here. However, for FA at 25 °C, the reported τ_{sm} = 5.4 ps from NMR[30] enables us to conclude that $g_2 \approx 2.4$. This in turn suggests that strong orientational pair correlations exist between the anisotropic polarizabilities of adjacent FA molecules in the liquid. Therefore, orientational correlations as well as boundary conditions and shape effects may play a role here in determining the slope of the $\langle\tau\rangle$ versus η/T plot (Figure 5). However, the fact that the slope of $\langle\tau\rangle$ against η/T is less for the solutions than for pure FA suggests that at least one of these factors is affected differently by increasing ion concentration, suggesting a change in the mechanism underpinning orientational relaxation between pure FA and the solutions.

We note that the differential effect of NaI and KI is not evident at low concentration ($c \leq 1.3$ M, corresponding to $10^3\eta/T \leq 16$ cP K^{-1}), in line with previous results of DRS experiments on alkali metal halide–FA solutions.[35,73] This indicates that the effect of different ionic species on solvent reorientation dynamics at these low concentrations is mainly through the perturbation of the liquid viscosity.[35,73] However, at higher concentration, the data diverge from a common trend and from linear behavior. The strongest deviation is observed for the NaI–FA solution, which implies a larger correction to the SED model by virtue of a cation-related effect (Na^+ has higher charge density hence a greater extent of solvation than K^+).

The stretching parameter β of the fitting exponential decreases upon increasing Na/KI concentration (Table 2a). A decrease in β is also produced by a decreasing temperature of the pure solvent (Table 2b), although to a lesser extent than for increasing ion concentration. In both cases, this indicates a greater deviation from a single-exponential behavior, or a broader distribution of relaxation times, as new ion–molecule or more H-bonding interactions occur. Evidently, there is a greater dispersion in the relaxation times in the concentrated salt solutions than in the cooled neat liquid.

3.2. Ultrafast Dynamics. After subtraction of the diffusive contribution, the oscillatory features at very short time scales (Figure 1; inset) were analyzed in the frequency domain (Figure 3). It can be seen (Supporting Information, Figure SI-3) that the subtraction of the diffusive (stretched exponential) part of the dynamics removes an intense peak at the lowest frequencies of the RSD of liquid FA to more clearly reveal the three remaining components in the rRSD.

While the slow dynamics in the Kerr decay of liquids are primarily related to diffusive molecular reorientation, here affected by H-bonding, the ultrafast portion of the decay is generally associated with coherently excited hindered molecular rotations or vibrations—otherwise referred to as *librations*—and intermolecular interaction-induced (II) effects. The rRSD of liquid FA presents a structured profile, having three main features which have been related to II and two librational contributions.[33] The assignment of the low-frequency II contributions to the depolarized spectral density is challenging in the absence of polarization resolved data, as additional

dx.doi.org/10.1021/jp3087418 | J. Phys. Chem. B 2012, 116, 13481–13489

molecular librations may also contribute.[32,74] However, isotropic OKE measurements suggest that II effects may contribute at lower frequencies than librations in some cases, depending on the molecular shape.[55,75,76] As a consequence of this uncertainty, it is difficult to make a conclusive assignment of the lowest frequency ohmic component. The two Gaussian librational components at ∼190 and 90 cm^{-1} have been related to different dimensionality of H-bonding structures in liquid FA[21−23] (see below). The rRSD are shown in Figure 6 for

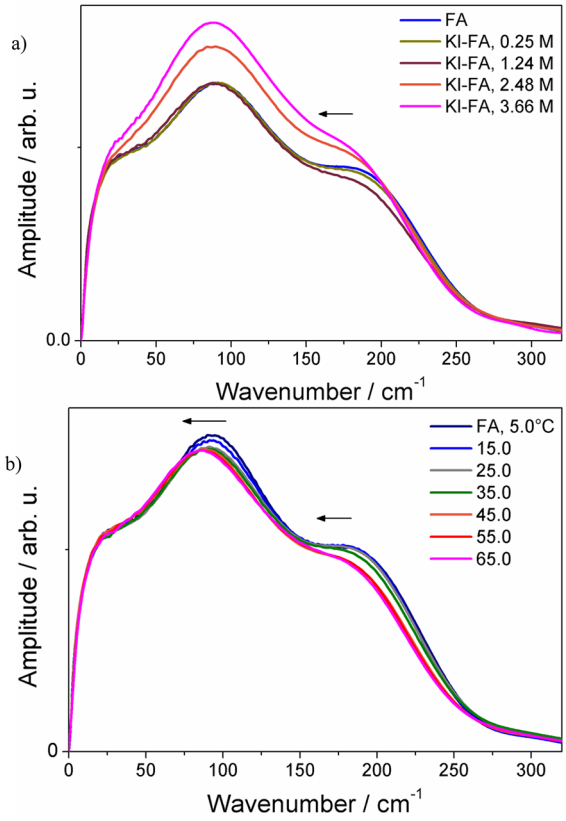

Figure 6. Evolution of the rRSD of (a) KI−FA solution as a function of concentration, in a range up to 3.7 M, and (b) pure FA as a function of temperature, in the range 5.0−65.0 °C. Spectra were normalized to the intensity at lower frequencies, where only slight changes are observed. Arrows indicate the direction of the observed shifts with increasing concentration/temperature of the sample.

increasing concentrations of KI and increasing temperature. Qualitatively, increasing temperature produces a small red shift of both the librational bands (Figure 6b), while increasing KI (and NaI; see Supporting Information, Figure SI-5a) concentration gives rise to a red shift of the high-frequency band, and little effect on the intermediate band (Figure 6a and Figure SI-5a).

Each rRSD was analyzed quantitatively by a multicomponent fit, using a sum of an ohmic and two antisymmetrized Gaussians (Figure 3, and Figure SI-5b in the Supporting Information). The resulting parameters for all solutions are listed in Supporting Information, Table SI-I. The two Gaussian components (assigned to librations of different H-bonding geometries[21,22]) are well separated and account for the major part of the rRSD intensity, and can thus be accurately fit. First, concerning the peak positions, both G_1 and G_2 red shift (by ∼9 and 12 cm^{-1}, respectively) with increasing temperature of the pure solvent (Figure 7b). Such a red shift is in line with a decreasing density of the system,[77] as previously observed for other H-bonded[78,79] and non-H-bonded liquids.[60] The physical origin is probably a weaker restoring force arising from greater molecular separation or weaker H-bonds. In contrast, both G_1 and G_2 red shift slightly upon increasing NaI concentration, while for increasing KI concentration, G_2 red shifts by ∼12 cm^{-1} (Figure 7a). Interestingly, the shift in G_2 is smaller for NaI than for KI, hence recalling the differential cation effect that was observed in the mean relaxation time and viscosity dependence (Figure 4). Here, the band red shift is paralleled by an *increase* of density as the NaI or KI concentration increases (Table 1 and Supporting Information, Figure SI-2); therefore, it is the opposite trend to that observed for the pure liquid FA versus temperature. This indicates that an ion-induced perturbation to the H-bonding structure gives rise to changes in the spectral density of the solution, rather than the density effect in pure FA. This again points to the different behavior seen with changing temperature compared to MX concentration.

Next, concerning the bandwidth, G_1 shows minor changes with temperature (Figure 7d), while G_2 progressively broadens (by up to ∼10 cm^{-1}), an effect that has been observed before and attributed to the large anharmonicity of the modes at these high frequencies.[5] Spectral changes observed here denote a stronger temperature effect on G_2 than G_1 for pure FA as was previously reported by Nielsen et al.[5] Regarding the ion effect, G_2 broadens by 6−7 cm^{-1} with increasing NaI and KI concentration (Figure 7c), which is slightly less than with increasing temperature of the pure liquid. However, the width of G_1 is rather constant for the KI solution and broadens by ∼11 cm^{-1} for the NaI solution, again reflecting a difference in the (cation) effect for NaI and KI at these frequencies. Finally, in terms of amplitude (relative integrated intensity) of the bands, G_1 and G_2 show a minor effect of temperature (with G_2 only slightly growing above 35 °C, as G_1 decreases; Figure 7f). Similarly, a minor effect on the amplitude of G_1 and G_2 is produced by KI addition (Figure 7e), while G_1 increases and G_2 decreases slightly upon NaI addition, again revealing a cation-related effect.

Overall, it is possible to rationalize the effects observed on the librational bands of liquid FA as follows. The red shift of G_1 and G_2 with increasing temperature (T) in the pure solvent correlates with the decrease in density. A red shift of similar magnitude is seen for the effect of increasing T and KI concentration on G_2 but the density change is in the opposite direction. Thus, the mechanism of the shift is different between temperature and added ions. Further, the shift of G_1 is much smaller than for G_2 as a function of ion concentration, suggesting that one librational component is more influenced by the salt than the other. Finally, KI causes a bigger red shift in G_2 and a bigger increase in density than does NaI. This suggests a differential effect of the cation on the librational spectra. The broadening of G_2 results from both increasing T and salt concentration, while only G_1 broadens upon NaI addition, an effect which cannot be attributed to anharmonicity (affecting G_2).

Here, the ion effects on FA rRSD are accounted for by the same three band profiles as those of the pure solvent. The results obtained can be explained based on findings of theoretical calculations by Torii and Tasumi.[21,22] The authors assigned the Raman bands at ∼100 and 190 cm^{-1}—here G_1 and G_2, respectively—to a different dimensionality of the H-bonding in liquid FA. In particular, the presence of an H-bond to the *cis*-NH group of FA in cyclic (2D) dimers,

dx.doi.org/10.1021/jp3087418 | J. Phys. Chem. B 2012, 116, 13481−13489

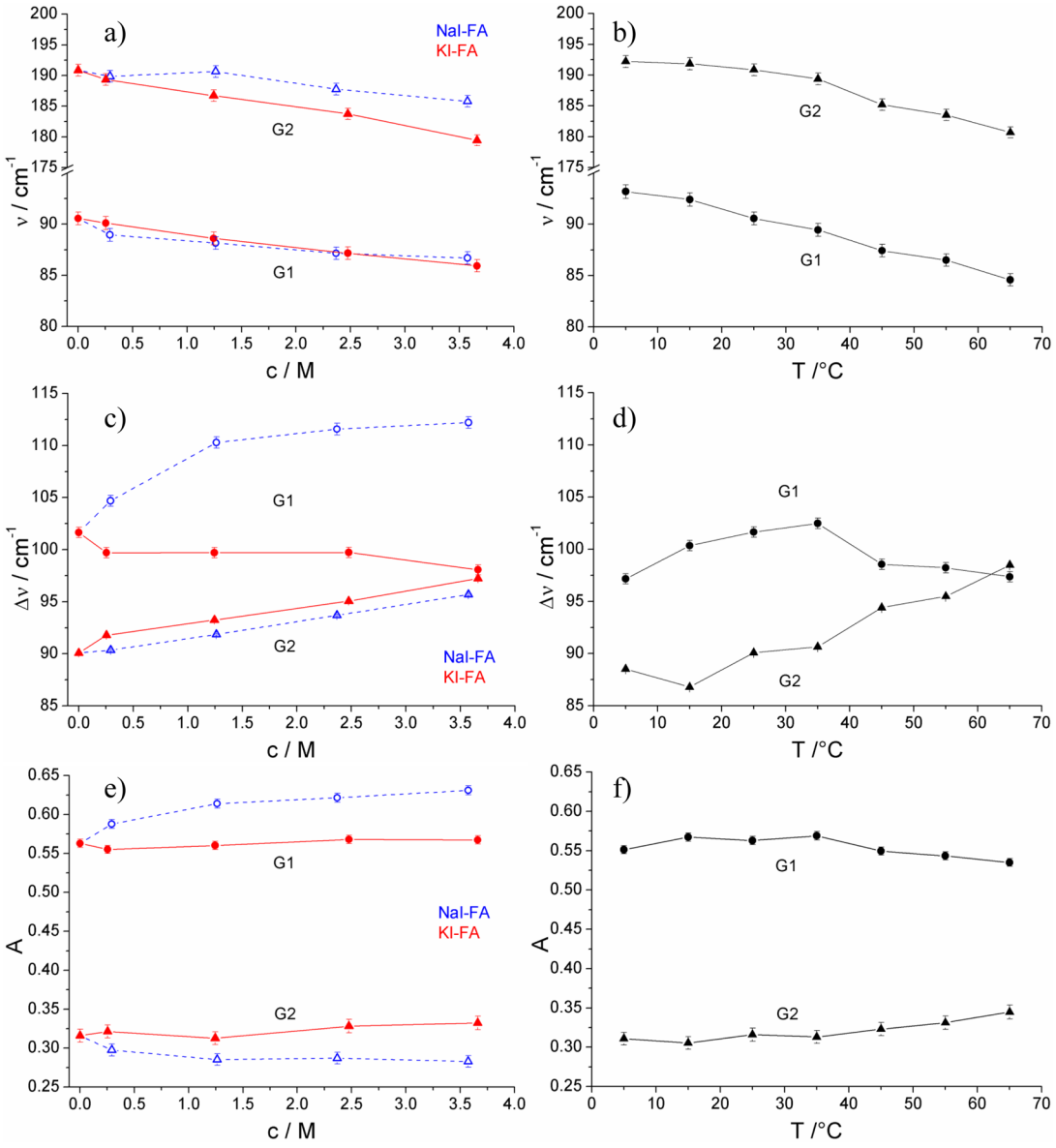

Figure 7. Results of a multicomponent fit applied to the rRSD of (a,c,e) NaI and KI–FA solutions at different concentration (blue, NaI; red, KI), and (b,d,f) pure FA at different temperatures. Reported values are as follows: characteristic frequency ν, bandwidth $\Delta\nu$, and relative amplitude A ($a_i/\sum a_n$, with a_i the integrated area in the range 0.03–400 cm^{-1}) of the two antisymmetrized Gaussians at ~90 cm^{-1} (G_1) and 190 cm^{-1} (G_2).

interconnected through *trans*-H-bonds in linear (1D) strands, exerts a resistance to the out-of-plane libration about the *z*-axis, which then results in a higher frequency than the less restricted libration of the *trans*-H-bonded molecules (~100 cm^{-1}).[22] The component at 190 cm^{-1}, which is not detected for *N*-methylformamide[22] and other FA analogues[45] or dipolar aprotic liquids,[60] is then peculiar to the two-dimensional structure of liquid FA. The spectrum of G_2 for the KI and NaI solutions as a function of increasing concentration (and density; Figure 6a, and Figure SI-5a in the Supporting Information) shows a reduction in this librational frequency, indicating disruption of the 2D H-bonds upon ion solvation. Increasing T of the pure liquid leads to a red shift of both librational bands (Figure 6b), but correlates with a decrease in density rather than the specific effect of ion solvation on the H-bond structure. The decreasing amplitude of the high-frequency band upon addition of NaI (Figure 7e) is indicative of a loss in two-dimensional structure of the liquid FA, accompanied by an increase of lower frequency 1D modes (G_1). Data were adequately fit by the same three functions used for neat FA. It is, however, plausible that cation–molecule interactions contribute through new bands, which might then be related to the increase in amplitude of G_1.[6]

It has been shown that Na^+–solvent interactions are stronger than bulk solvent interactions in FA.[80] The present results reveal a cation effect on librational dynamics and on the structure of liquid FA (specifically a perturbation of the 2D structure) which is stronger for NaI than KI, possibly by virtue of a bigger charge-to-size ratio ($Na^+ > K^+$). Note that a cation effect in this and other solvents has previously been revealed by analyzing the solvation dynamics.[81] The effects of LiI and other salts at lower concentration (Supporting Information, Table SI–I) are not substantial compared to those of NaI and KI as a function of concentration. However, most of these spectra also show a decrease in the frequency of the high-frequency band (Supporting Information, Figure SI-4) associated with the 2D

dx.doi.org/10.1021/jp3087418 | J. Phys. Chem. B 2012, 116, 13481–13489

structure of the liquid; this thus appears as a common feature to these alkali metal halide−FA solutions, although those containing lithium cation (Figure SI-4b) prove to be an interesting exception.

4. CONCLUSIONS

Optical Kerr effect spectroscopy was used to study both picosecond orientational dynamics and the low-frequency Raman spectra arising from librational modes of alkali metal halide−FA solutions. In particular, NaI and KI solutions were investigated over a wide range of concentrations, up to near saturation. "Free" monatomic ion reorientations are not Raman-active; however, their effect on the solvation shell molecules of FA compared to the bulk solvent can be detected. Changes due to ion solvation (ion−molecule interactions) were observed through the slowing down of FA reorientation which correlated with an increase in viscosity. The relaxation scaled with viscosity, but the scaling factor was different from that seen for the temperature-dependent reorientation, suggesting different factors controlled the relaxation in the solution. This was supported by the observation of a specific cation dependence ($Na^+ > K^+$) and increasingly dispersive relaxation dynamics with increasing ion concentration.

The rRSD was derived for all samples and analyzed with a three-component fit. As for the orientational relaxation time, the ultrafast librational dynamics of the liquid FA are determined by H-bonding effects. Addition of salt to FA has the effect of red-shifting the highest librational frequencies. A similar shift is observed with an increase of temperature for the pure liquid. However, opposite changes in density are observed in these two cases and ions preferentially affect one librational band more strongly than the other. This can be explained based on previous MD simulation results which assign the two bands to different dimensionality of H-bonding in the liquid. The red shift of the bands is thus related to a disruption of the H-bond structure in FA. With NaI addition accounting for bigger G_1 amplitude than KI, we conclude that the smaller cation, with stronger charge density, has the greater effect on FA structure and dynamics.

■ ASSOCIATED CONTENT

Supporting Information

Time and spectral domain data of a range of ionic FA solutions at fixed concentration. This material is available free of charge via the Internet at http://pubs.acs.org.

■ AUTHOR INFORMATION

Corresponding Author

*E-mail: s.meech@uea.ac.uk.

Notes

The authors declare no competing financial interest.

■ ACKNOWLEDGMENTS

This project was funded by EPSRC grants EP/H025715. The authors gratefully acknowledge Dr. Kamila Mazur for her support in the experiments.

■ REFERENCES

(1) Nandi, P. K.; Robinson, D. R. *J. Am. Chem. Soc.* **1972**, *94*, 1299−1308.
(2) DeSando, R.; Brown, G. *J. Phys. Chem.* **1968**, *72*, 1088−1091.
(3) Chen, T.; Hefter, G.; Buchner, R.; Senanayake, G. *J. Solution Chem.* **1998**, *27*, 1067−1096.
(4) Siegbarn, H.; Asplund, L.; Kelfve, P.; Hamrin, K.; Karlsson, L.; Siegbahn, K. *J. Electron Spectrosc.* **1974**, *5*, 1059−1079.
(5) Nielsen, O. F.; Lund, P.-A.; Praestgaard, E. *J. Chem. Phys.* **1982**, *77*, 3878−3883.
(6) Nielsen, O. F.; Christensen, D. H.; Rasmussen, O. H. *J. Mol. Struct.* **1991**, *242*, 273−282.
(7) Ohtaki, H.; Funaki, A.; Rode, B. M.; Reibnegger, G. J. *Bull. Chem. Soc. Jpn.* **1983**, *56*, 2116−2121.
(8) Miyake, M.; Kaji, O.; Nakagawa, N.; Suzuki, T. *J. Chem. Soc., Faraday Trans. 2* **1985**, *81*, 277−281.
(9) Wiesmann, F. J.; Zeidler, M. D.; Bertagnolli, H.; Chieux, P. *Mol. Phys.* **1986**, *57*, 275−285.
(10) Hippler, M.; Hertz, H. G. *Z. Phys. Chem.* **1992**, *175*, 25−39.
(11) Ludwig, R.; Weinhold, F.; Farrar, T. C. *J. Chem. Phys.* **1995**, *102*, 5118−5125.
(12) Bellissent-Funel, M.-C.; Nasr, S.; Bosio, L. *J. Chem. Phys.* **1997**, *106*, 7913−7919.
(13) Jadzyn, J.; Swiergiel, J. *Phys. Chem. Chem. Phys.* **2012**, *14*, 3170−3175.
(14) Jorgensen, W. L.; Swenson, C. J. *J. Am. Chem. Soc.* **1985**, *107*, 569−578.
(15) Essex, J. W.; Jorgensen, W. L. *J. Phys. Chem.* **1995**, *99*, 17956−17962.
(16) Sagarik, K. P.; Ahlrichs, R. *J. Chem. Phys.* **1987**, *86*, 5117−5126.
(17) Puhovski, Y. P.; Rode, B. M. *Chem. Phys.* **1995**, *190*, 61−82.
(18) Puhovski, Y. P.; Safonova, L. P.; Rode, B. M. *J. Mol. Liq.* **2003**, *103−104*, 15−31.
(19) Cordeiro, J. M. M. *Int. J. Quantum Chem.* **1997**, *65*, 709−717.
(20) Richardi, J.; Krienke, H.; Fries, P. H. *Chem. Phys. Lett.* **1997**, *273*, 115−121.
(21) Torii, H.; Tasumi, M. *Int. J. Quantum Chem.* **1998**, *70*, 241−252.
(22) Torii, H.; Tasumi, M. *J. Phys. Chem. A* **2000**, *104*, 4174−4181.
(23) Torii, H. *Chem. Phys. Lett.* **2002**, *353*, 431−438.
(24) Tsuchida, E. *J. Chem. Phys.* **2004**, *121*, 4740−4746.
(25) Radnai, T.; Megyes, T.; Bakó, I.; Kosztolányi, T.; Pálinkás, G.; Ohtaki, H. *J. Mol. Liq.* **2004**, *110*, 123−132.
(26) Elola, M. D.; Ladanyi, B. M. *J. Chem. Phys.* **2006**, *125*, 184506.
(27) Elola, M. D.; Ladanyi, B. M. *J. Chem. Phys.* **2007**, *126*, 084504.
(28) Bako, I.; Megyes, T.; Balint, S.; Chihaia, V.; Bellissent-Funel, M.-C.; Krienke, H.; Kopf, A.; Suh, S.-H. *J. Chem. Phys.* **2010**, *132*, 014506.
(29) Weingärtner, H.; Holz, M.; Hertz, H. G. *J. Solution Chem.* **1978**, *7*, 689−704.
(30) Holz, M.; Rau, C. K. *J. Chem. Soc., Faraday Trans. 1* **1982**, *78*, 1899−1910.
(31) Whittenburg, S. L.; Jain, V. K.; McKinnon, S. J. *J. Phys. Chem.* **1986**, *90*, 1004−1005.
(32) Chang, Y. J.; Castner, E. W. *J. Chem. Phys.* **1993**, *99*, 113−125.
(33) Chang, Y. J.; Castner, E. W. *J. Phys. Chem.* **1994**, *98*, 9712−9722.
(34) Barthel, J.; Buchner, R.; Wurm, B. *J. Mol. Liq.* **2002**, *98−99*, 51−69.
(35) Wurm, B.; Baar, C.; Buchner, R.; Barthel, J. *J. Mol. Liq.* **2006**, *127*, 14−20.
(36) Puhovski, Y. P.; Rode, B. M. *J. Chem. Phys.* **1995**, *102*, 2920−2927.
(37) Buchner, R. *Pure Appl. Chem.* **2008**, *80*, 1239−1252.
(38) Park, K.-H.; Choi, S. R.; Choi, J.-H.; Park, S.; Cho, M. *ChemPhysChem* **2010**, *11*, 3632−3637.
(39) Ladell, J.; Post, B. *Acta Crystallogr.* **1954**, *7*, 559−564.
(40) Itoh, K.; Shimanouchi, T. *J. Mol. Spectrosc.* **1972**, *42*, 86−99.
(41) Green, J. L.; Lacey, A. R.; Sceats, M. G. *J. Phys. Chem.* **1986**, *90*, 3958−3964.
(42) Bukowska, J. *Chem. Phys. Lett.* **1978**, *57*, 624−626.
(43) Nielsen, O. F.; Lund, P. A. *Chem. Phys. Lett.* **1981**, *78*, 626−628.
(44) Nielsen, O. F.; Bigio, I. J.; Olsen, I.; Berquier, J. M. *Chem. Phys. Lett.* **1986**, *132*, 502−506.

(45) Hunt, N. T.; Turner, A. R.; Tanaka, H.; Wynne, K. *J. Phys. Chem. B* **2007**, *111*, 9634−9643.
(46) McMorrow, D.; Lotshaw, W. T.; Kenneywallace, G. A. *IEEE J. Quantum Electron.* **1988**, *24*, 443−454.
(47) Righini, R. *Science* **1993**, *262*, 1386−1390.
(48) Smith, N. A.; Meech, S. R. *Int. Rev. Phys. Chem.* **2002**, *21*, 75−100.
(49) Zhong, Q.; Fourkas, J. T. *J. Phys. Chem. B* **2008**, *112*, 15529−15539.
(50) Heisler, I. A.; Meech, S. R. *Science* **2010**, *327*, 857−860.
(51) Heisler, I. A.; Mazur, K.; Meech, S. R. *J. Phys. Chem. B* **2011**, *115*, 1863−1873.
(52) http://webbook.nist.gov/chemistry/.
(53) Hunt, N. T.; Jaye, A. A.; Meech, S. R. *Phys. Chem. Chem. Phys.* **2007**, *9*, 2167−2181.
(54) Garduno-Mejia, J.; Meech, S. R. *Opt. Commun.* **2006**, *259*, 840−847.
(55) Heisler, I. A.; Meech, S. R. *J. Phys. Chem. B* **2008**, *112*, 12976−12984.
(56) Mazur, K.; Heisler, I. A.; Meech, S. R. *J. Phys. Chem. B* **2010**, *114*, 10684−10691.
(57) Turton, D. A.; Wynne, K. *J. Chem. Phys.* **2009**, *131*, 201101.
(58) Hinze, G.; Francis, R. S.; Fayer, M. D. *J. Chem. Phys.* **1999**, *111*, 2710−2719.
(59) McMorrow, D.; Lotshaw, W. T. *J. Phys. Chem.* **1991**, *95*, 10395−10406.
(60) Palombo, F.; Paolantoni, M.; Sassi, P.; Morresi, A.; Giorgini, M. G. *Phys. Chem. Chem. Phys.* **2011**, *13*, 16197−16207.
(61) Greenfield, S. R.; Sengupta, A.; Stankus, J. J.; Fayer, M. D. *Chem. Phys. Lett.* **1992**, *193*, 49−54.
(62) Smith, N. A.; Meech, S. R. *J. Phys. Chem. A* **2000**, *104*, 4223−4235.
(63) Ricci, M.; Bartolini, P.; Chelli, R.; Cardini, G.; Califano, S.; Righini, R. *Phys. Chem. Chem. Phys.* **2001**, *3*, 2795−2802.
(64) Shirota, H.; Fujisawa, T.; Fukazawa, H.; Nishikawa, K. *Bull. Chem. Soc. Jpn.* **2009**, *82*, 1347−1366.
(65) Frey, J. A.; Leutwyler, S. *J. Phys. Chem. A* **2006**, *110*, 12512−12518.
(66) Taniewska-Osinska, S.; Piekarska, A.; Kacperska, A. *J. Solution Chem.* **1983**, *12*, 717−727.
(67) Jenkins, H. D. B.; Marcus, Y. *Chem. Rev.* **1995**, *95*, 2695−2724.
(68) Marcus, Y. *Chem. Rev.* **2009**, *109*, 1346−1370.
(69) Corridoni, T.; Mancinelli, R.; Ricci, M. A.; Bruni, F. *J. Phys. Chem. B* **2011**, *115*, 14008−14013.
(70) Martinus, N.; Vincent, C. A. *J. Chem. Soc., Faraday Trans. 1* **1981**, *77*, 141−146.
(71) Dote, J. L.; Kivelson, D.; Schwartz, R. N. *J. Phys. Chem.* **1981**, *85*, 2169−2180.
(72) Kivelson, D.; Madden, P. A. *Annu. Rev. Phys. Chem.* **1980**, *31*, 523−558.
(73) Barthel, J.; Buchner, R.; Bachhuber, K.; Hetzenauer, H.; Kleebauer, M.; Ortmaier, H. *Pure Appl. Chem.* **1990**, *62*, 2287−2296.
(74) Manfred, K.; He, X.; Fourkas, J. T. *J. Phys. Chem. B* **2010**, *114*, 12096−12103.
(75) Heisler, I. A.; Meech, S. R. *J. Chem. Phys.* **2010**, *132*, 174503.
(76) Ryu, S.; Stratt, R. M. *J. Phys. Chem. B* **2004**, *108*, 6782−6795.
(77) Dunn, L. A.; Stokes, R. H. *Trans. Faraday Soc.* **1969**, *65*, 2906−2912.
(78) Paolantoni, M.; Sassi, P.; Palombo, F.; Morresi, A.; Paliani, G.; Cataliotti, R. S. *Proceedings of GNSR 2003 Conference*; Morresi, A., Sassi, P., Eds.; Morlacchi, Perugia, Italy, 2004; pp 18−26.
(79) Sassi, P.; Paolantoni, M.; Perticaroli, S.; Palombo, F.; Morresi, A. *J. Raman Spectrosc.* **2009**, *40*, 1279−1283.
(80) Puhovski, Y. P.; Rode, B. M. *Chem. Phys.* **1997**, *222*, 43−57.
(81) Chapman, C. F.; Maroncelli, M. *J. Phys. Chem.* **1991**, *95*, 9095−9114.